Biomarkers, 2009; 14(6): 372–380

informa
healthcare

RESEARCH ARTICLE

Metabonomic characterization of early atherosclerosis in hamsters with induced cholesterol

Weibin Zha[1], Jiye A[1], Guangji Wang[1], Bei Yan[1], Shenghua Gu[1], Xuanxuan Zhu[2], Haiping Hao[1], Qing Huang[1], Jianguo Sun[1], Ying Zhang[1], Bei Cao[1], and Hongcan Ren[1]

[1]*Key Laboratory of Drug Metabolism and Pharmacokinetics, China Pharmaceutical University, Nanjing, China, and* [2]*Department of Pharmacology, Clinical Research Institute of Jiangsu Provincial Hospital of Traditional Chinese Medicine, Nanjing, China*

Abstract

Atherosclerosis is a complicated and multifactorial disease, induced not only by genotype, but also, even more importantly, by environmental factors. Study on the metabolic perturbation of endogenous compounds may offer deeper insight into development of atherosclerosis. Gas chromatography/mass spectrometry (GC/MS)-based metabonomics was used to profile a metabolic fingerprint of serum obtained from hamsters with induced cholesterol. The deconvoluted GC/MS data were processed by multivariate statistical analysis tools, such as principal component analysis (PCA) and partial least squares projection to latent structure and discriminant analysis (PLS-DA). For the first time we showed a time-dependent development of the model animal from normal to hypercholesterolaemia, and further to early atherosclerosis. Twenty-one compounds were identified as markers involved in the development to atherosclerosis. Identification of the compounds suggests that amino acid metabolism and fatty acid oxidation are significantly perturbed following cholesterol overloading. The data provide novel information to approach the pathophysiological processes of the hypercholesterolaemia and atherosclerosis disease continuum.

Keywords: *Metabonomics; early atherosclerosis; hypercholesterolaemia; GC/MS; multivariate statistical analysis*

Introduction

Atherosclerosis is a chronic progressive disease, which is also the primary cause of cardiovascular disease and stroke. It is estimated that atherosclerosis and its related diseases account for approximately 50% of all deaths in developed countries (Lusis 2003, Lahoz & Mostaza 2007). Hypercholesterolaemia is thought to be an important initiating factor of atherosclerosis, and it even triggers induction of fatty streak lesions, the earliest visible lesions of atherosclerosis (Steinberg et al. 2002). Unfortunately, the complex pathophysiology of atherogenesis still remains largely unknown despite a decade of research. Novel methods are in great demand to provide deeper insight into the processes initiated by hypercholesterolaemia.

To date, genomics, transcriptomics and proteomics have been applied to investigate complicated diseases (Tuomisto et al. 2005, Bijnens et al. 2006, Sung et al. 2006). However, there is an increasing recognition of the limitations of approaches that do not take into account the important environmental influences; atherosclerosis is induced not only by genotype, but also by environmental factors such as a high-fat diet, smoking and even drug side-effects (Lahoz & Mostaza 2007, Kleemann et al. 2007, Hui 2003). Considering the well-known impact of food and environment on the development of atherosclerosis, metabonomic investigations may

Address for Correspondence: Guangji Wang, Key Laboratory of Drug Metabolism and Pharmacokinetics, China Pharmaceutical University, 1 Shennong Road, Nanjing 210038, China. Tel.: +86-25-8327 1128. Fax: +86-25-8530 6750. E-mail: guangjiwang@hotmail.com
Weibin Zha and Jiye A are joint first authors.

(Received 11 November 2008; accepted 07 May 2009)

ISSN 1354-750X print/ISSN 1366-5804 online © 2009 Informa UK Ltd
DOI: 10.1080/13547500903026401

provide valuable information on the endogenous molecules involved in metabolic perturbation and hence deeper insight into the disease.

Metabonomics was originally defined by Nicholson et al. (1999) as the quantitative measurement of the multiparametric metabolic response of living systems. Using high-throughput analytical tools, such as ^{1}H nuclear magnetic resonance (NMR), gas chromatography/time-of-flight mass spectrometry (GC/TOF-MS), and liquid chromatography (LC)/MS in combination with principal component analysis (PCA), a large number of endogenous metabolites can be determined to clarify the intrinsic differences between biosamples. By means of these powerful tools, metabonomics has demonstrated its potential in many fields, such as diagnosis of disease, biomarker discovery and exploration of pathogenesis (Yi et al. 2008, Kenny et al. 2005, Dumas et al. 2006). Brindle and the colleagues (2002) completed a pioneering metabonomic study on diagnosing the presence and severity of coronary heart disease using proton NMR spectra. In a recent metabonomic study, novel biomarkers of acute myocardial ischaemia were identified based on LC (Sabatine et al. 2005). Another study focused on the gene-related metabolic variations of atherosclerosis in apolipoprotein $E^{-/-}$ mice using proteomic and metabolomic analyses (Mayr et al. 2005). These studies suggest metabonomics are a potentially useful approach to exploring atherosclerosis, but the metabolic variation along with the development of atherosclerosis induced by high-fat food has not been clarified. Therefore, this study focuses on characterizing the processes from hypercholesterolaemia to early atherosclerosis in LVG Syrian hamsters fed with a high-cholesterol diet. Serum from the hamsters was collected and analysed based on the GC/TOF-MS technology developed by Jonsson et al. (2005) and A et al. (2005).

Materials and methods

Chemicals

All the reference compounds were purchased from Sigma (St Louis, MO, USA), Merck (Darmstadt, Germany), Aldrich (Steinhein, Germany) and Serva (Heidelberg, Germany), and were of analytical grade except where specifically designated. Methoxyamine hydrochloride and the stable isotope-labelled internal standard compounds (IS), ($^{13}C_2$)-myristic acid, were purchased from Sigma-Aldrich. Alkane series (C_8 to C_{40}) and pyridine (silylated grade) were obtained from Fluka (Buchs, Switzerland). *N*-methyl-*N*-trimethylsilyltrifluoroacetamide (MSTFA) plus 1% trimethylchlorosilane (TMCS) were purchased from Pierce Chemical Company (Rockford, IL, USA); heptane purchased from TEDIA (Fairfield, OH, USA) is of high-performance LC (HPLC) grade. Distilled water was produced by a Milli-Q Reagent Water System (Millipore, Bedford, MA, USA).

Experimental animal model

A total of 24 male LVG Syrian hamsters aged 8 weeks were obtained from Vital River Lab Animal Technology Co., Ltd (Peking, China) and the experimental protocol was approved by the Animal Ethics Committee of China Pharmaceutical University. The animals were housed in hanging polystyrene cages with a layer of sawdust as bedding in a controlled environment (22 ± 1°C, 50 ± 20% relative humidity and a 12 h light/12 h dark cycle). All diets and water were provided *ad libitum*. Hamsters were fed with a standard diet (crude protein, 190 g kg^{-1}; crude fat, 70 g kg^{-1}; crude fibre 30 g kg^{-1}; calcium, 16 g kg^{-1}; phosphonium, 12 g kg^{-1}) for 2 weeks for acclimation. They were then randomized into three experimental groups of eight animals each based on body weight. During the 12-week experimental period, the control group (Con) was continued on the standard diet, the high-cholesterol group (HC) was fed a hypercholesterolaemic diet (HCD) consisting of additions of 10% w/w coconut oil and 0.3% w/w cholesterol, and the extra-high-cholesterol group (EHC) was fed the HCD with additions of 10% w/w coconut oil and 0.8% w/w cholesterol. Clinical examination and measurement of body weight were performed once a week and food consumption was recorded during 6 consecutive days at weeks 4 and 8 of the study. Retro-orbital bleeds were performed pre-dose and at baseline, and at 6, 9 and 12 weeks. The blood was allowed to clot for 2 h and the serum was collected by centrifugation at 1600*g* for 10 min. Each serum sample was divided into two parts, one for immediate serum lipid determination and the other kept at –80°C for GC/MS analysis.

Serum lipid analysis

Total serum cholesterol (TC) (Allain et al. 1974) and triglyceride (TG) (Bucolo & David 1973) concentrations were measured enzymatically. Low-density lipoprotein cholesterol (LDL-C) was measured using phosphotungstate reagent (Weingand & Daggy 1990), and high-density lipoprotein cholesterol (HDL-C) was measured in the supernatant. All determinations were carried out on an Olympus-AU2700 Bichromatic autoanalyzer (Olympus, Tokyo, Japan) in Jiangsu Provincial Hospital of Traditional Chinese Medicine.

Foam cell assessment

At the end of the experiments, animals were sacrificed under anaesthesia. The hearts were removed (with attached thoracic aorta) and stored in 10% neutral buffered formalin at 4°C until analysis. Prior to foam cell

quantitation, the aortic arch was separated from the heart immediately superior to the aortic valve. Sections of the aorta between the third neck vessel and 1 mm above the aortic valve were stained with Sudan III. The stained arches were opened longitudinally and mounted flat on a glass slide with a glass coverslip, and photographed using an Olympus BX60 brightfield microscope (Olympus Optical Co., Tokyo, Japan). The microscopic images were captured with an Olympus DP71 digital camera (Olympus, Tokyo, Japan). The total foam cell area (the summary of all Sudan III-stained fatty particle areas in the foam cells) was analysed with Image-Pro Plus 6.0 software (Media Cybernetics, Bethesda, MD, USA). Measurements are expressed as μm^2 foam cell area per mm^2 aorta arch area.

Sample extraction and GC/MS analysis

The hamster serum was analysed as previously described (A et al. 2005) with some modification. In brief, to each serum sample (100 μl), 400 μl methanol with 2 μg ($^2C_{13}$)-myristic acid was added in an Eppendorf tube as the internal standard. The tube was vigorously vortexed for 5 min and placed at 0°C for 1 h, then centrifuged at 19 600*g* for 5 min. One hundred microlitres of the resulting supernatant was transferred to a GC vial, and evaporated to dryness in a Speed-vac Concentrator (Savant Instrument, Framingdale, NY, USA). Thirty microlitres of methoxyamine (10 μg μl^{-1}) in pyridine was added to each GC vial, and vigorously vortexed for 5 min. Methoxymation was carried out at room temperature for 16 h. The solution was then vortexed again for 2 min after adding 30 μl MSTFA with 1% TMCS as the catalyst. After trimethylsilylation for 1 h, 30 μl of heptane with methyl myristate as QC reference standard at 30 μg ml^{-1} was added into each GC vial.

A 1 μl aliquot of each sample was injected splitless by an Agilent 7683 Series Autosampler (Agilent, Atlanta, GA, USA) into an Agilent 6980 GC equipped with a 10 m × 0.18 mm ID, fused silica capillary column chemically bonded with 0.18 μm DB5-MS stationary phase (J&W Scientific, Folsom, CA, USA). The oven temperature was initially kept at 70°C for 2 min, then increased from 70 to 305°C at 35°C min^{-1}, where it was held for 2 min. Other instrumental parameters were as follows: the injector temperature and the transfer line temperature all at 250°C, the electron energy at 70 eV and the ion source temperature at 200°C. Helium, as a carrier gas, was set at a constant flow rate of 1 ml min^{-1} through the column. For every analysis, the septum purge flow rate was 20 ml min^{-1}, and the purge was turned on after 1 min. The column effluent was introduced into the ion source of a Pegasus III MS (Leco Corp., St Joseph, MI, USA). All data were collected in the mass from 50 to 800 *m/z* at a rate of 20 spectra s^{-1}, and the acceleration voltage was turned on after a solvent delay of 175 s.

ChromaTOF™ 2.00 software (Leco Corp.) was used for automated mass spectral deconvolution and peak identification with the peak width set to 2 s. Peaks with signal-to-noise (S/N) ratios higher than 30 were accepted. To obtain accurate peak areas for the internal standard and specific peaks/compounds, one quant mass was specified for each peak and the data were reprocessed as described previously (Jonsson 2007, A et al. 2005). Before identification, the retention index of each peak was calculated against alkane series C8-C40, analysed with the same GC program. The compounds were identified either by comparison of the mass spectra and retention index of all the detected compounds with their reference standards or those available in the database of the National Institute of Standards and Technology (NIST) library 2.0 (2005), the Wiley library, and an in-house mass spectra library database established by the Umeå Plant Science Center, Swedish University of Agricultural Sciences, and the Key Laboratory of Drug Metabolism and Pharmacokinetics, China Pharmaceutical University.

Data processing and pattern recognition

Multivariate statistical analysis (MVSA) was carried out using SIMCA-P 11 software (Umetrics, Umeå, Sweden). PCA and partial least squares projection to latent structure and discriminant analysis (PLS-DA) were employed to process the acquired GC/TOF-MS data, as described previously (Trygg & Lundstedt 2007, Eriksson et al. 2001). The results of the PCA were displayed as score plots to represent the scatter of samples; further metabolite differences were shown in PCA loading plots. When tightly clustered, these indicate similar metabolic phenotypes, and loosely clustered, they indicate compositionally different metabolic phenotypes. In the PLS-DA model, samples of the different groups were classified into different classes in score plots, and endogenous metabolites contributing to the classification were identified in loading plots, which showed the importance of each variable to the classification. Cross-validation with seven cross-validation groups was used throughout to determine the number of components (Wold 1978). The following statistics for the regression models are discussed throughout this paper. R^2X is the cumulative modelled variation in GC/MS response variables, *X*; R^2Y is the cumulative modelled variation in observation variables, *Y*; and Q^2Y is the cumulative predicted variation in *Y*, according to cross-validation. The ranges of these parameters are 0–1, where 1 indicates a perfect fit.

Statistical analysis was made using two-tailed Student's *t*-test by direct comparisons of biochemical parameters or relative metabolite abundance (peak areas normalized by the stable isotope internal standard), i.e. between the control group and the model groups. The level of statistical significance was set at $\alpha < 0.05$.

Results

Body weight and food intake

Before the experiments, no differences were observed in body weight among the groups (Con group, 115 ± 10.1 g; HC group, 116 ± 10.7 g; EHC group, 115 ± 10.0 g), but their weights increased through the experiments. Average food intake was 17.2 ± 3.10, 16.6 ± 0.74, 14.0 ± 2.00 g per 48 h for the Con, HC and EHC groups at week 4, and 15.0 ± 2.89, 14.2 ± 1.07, 14.2 ± 0.60 g per 48 h at week 8, respectively. For the Con and HC groups, food intake at week 4 was slightly higher than that at week 8, but was not statistically significant.

Measurement of serum lipids

At the end of the experiment (week 12), levels of TC, TG, HDL-C and LDL-C in the serum were significantly elevated in the hamsters fed both with the HC and EHC diet compared with the control (Figure 1A). For the cholesterol-fed groups, serum lipid in the HC group was significantly lower than in the EHC group (Figure 1A). In addition, no significant differences were found in serum lipid concentrations from week 6 to week 12 for any of the groups following cholesterol induction (data not shown).

Formation of foam cells

Aortic arches were inspected to score early atherosclerosis from animas in the Con, HC and EHC groups after 12 weeks of dietary treatment. Significant lesions/abnormalities were observed. The foam cells area measured in the HC group was 3844 ± 3479 $\mu m^2 mm^{-2}$, which was significantly lower than that found in the EHC group (11 545 ± 4184 $\mu m^2 mm^{-2}$; $p < 0.005$). No lesions were observed in the aortas of the control group hamsters. Figure 1B clearly shows the formation of foam cells for HC and EHC groups, and no foam cells were observed in the Con group. The area of the lesions was proportional to the cholesterol content in the food, indicating that higher cholesterol intake may result in a greater risk of atherosclerosis.

Metabolic perturbation of hamsters fed with lipid diet

A typical GC/MS fingerprint of serum is shown in Figure 2A. To investigate possible metabolic differences between the sample classes, the GC/MS data obtained were processed using a method described previously (Jonsson et al. 2005). A total of 119 peaks were resolved and the areas were obtained, 68 of which were identified. A PCA model did not show any serious outlier. Then a PLS-DA model of two principal components was calculated among the control group, HC group and EHC group at 6 and 12 weeks, respectively. We observed large variations within the HC and EHC groups at 6 weeks so that the PLS-DA did not differentiate the groups well (data not shown). However, the diverse diet treatments resulted in an excellent separation of the groups at 12 weeks (Figure 2B). This indicated significant diet-dependent differences of metabolic variations in hamster serum. The average distance between the HC

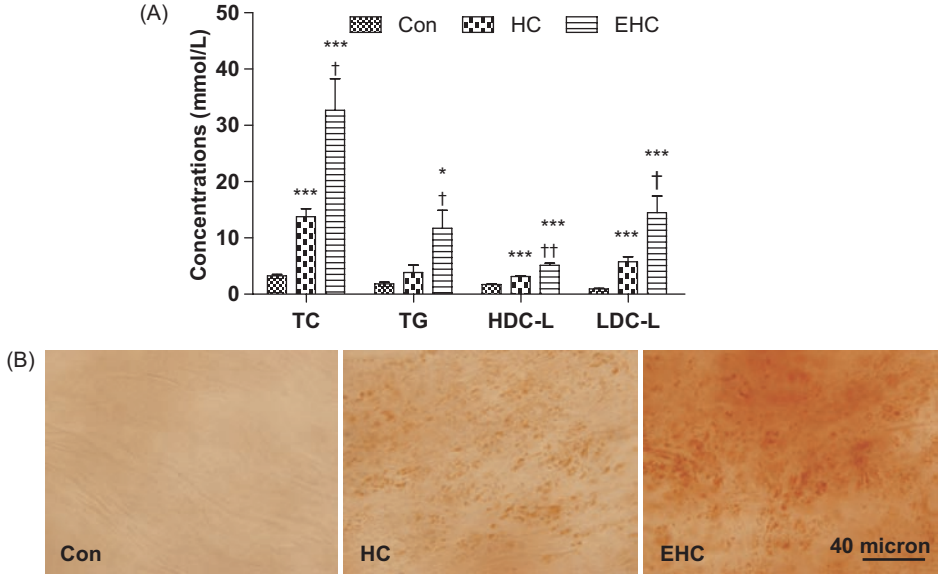

Figure 1. Measurement of serum lipids and atherosclerosis. (A) Lipoprotein profiles of the control (Con), high-cholesterol (HC) and extra-high-cholesterol (EHC) groups at week 12. TC, total cholesterol; TG, triglyceride; HDL-C, high-density lipoprotein cholesterol; LDL-C, low-density lipoprotein cholesterol. (B) Microscopic photographs of the endothelial aorta for the Con, HC and EHC groups at week 12. Foam cell areas were measured directly next to the mitric valves of hamsters. *$p < 0.05$, ***$p < 0.001$ vs Con; †$p < 0.05$, ††$p < 0.01$ vs HC (two-tailed Student's *t*-test).

samples and the controls was shorter than that between the EHC and the controls, indicating that metabolomic variation was positively correlated to the amount of cholesterol in the food and also the severity of early atherosclerosis. To investigate the variation in detail, the submodels were calculated respectively between the two groups. A clear separation was achieved between the controls and the model groups (Figure 2C–F).

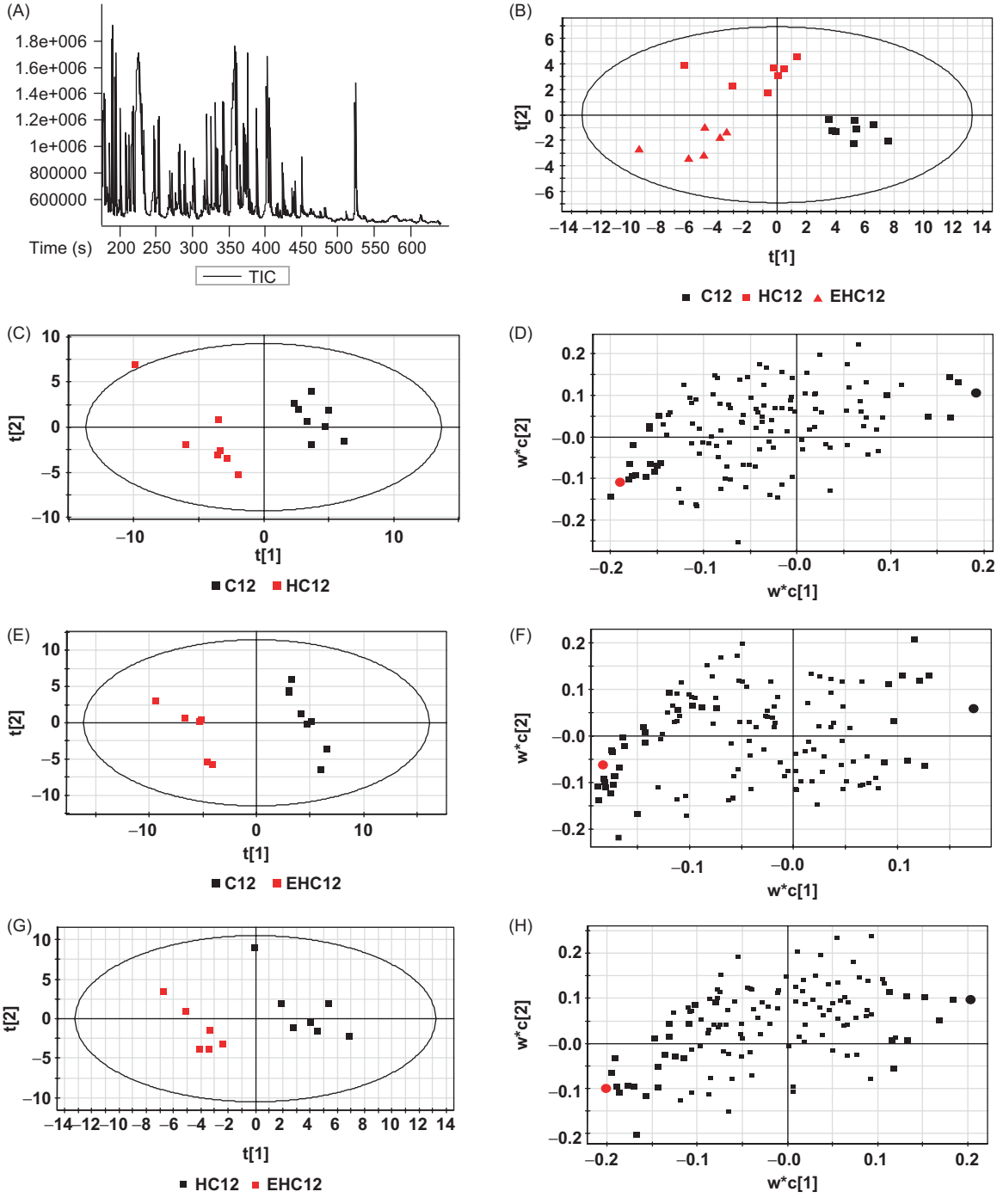

Figure 2. Gas chromatography/time-of-flight mass spectrometry (GC/TOF-MS) profiles of hamster serum and multivariate data analysis of the data. (A) GC/TOF-MS TIC fingerprint of hamster serum. (B) Partial least squares projection to latent structure and discriminant analysis (PLS-DA) score plots of the three groups (control (C), high-cholesterol (HC), extra-high-cholesterol (EHC)) at week 12 (two principal components (PCs), $R^2X=0.282$, $R^2Y=0.864$, $Q^2Y=0.478$). (C) PLS-DA score plot and (D) loading plot (right) between HC and control at week 12 (two PCs, $R^2X=0.328$, $R^2Y=0.946$, $Q^2Y=0.596$). (E) PLS-DA score plot and (F) loading plot between EHC and control at week 12 (two PCs, $R^2X=0.424$, $R^2Y=0.979$, $Q^2Y=0.596$). (G) PLS-DA score plot and (H) loading plot between EHC and HC at week 12 (two PCs, $R^2X=0.329$, $R^2Y=0.943$, $Q^2Y=0.350$).

In addition, good differentiation between the HC and EHC groups was also obtained as illustrated in the cross-validated score plots and loading plots of these samples (Figure 2G, H). The loading plots were made to display the specific compounds that differentiated between the three groups. A total of 21 identified metabolites were identified to characterize the metabolic profiles induced by increased cholesterol intake, summarized in Table 1.

In comparison with the control group, the groups fed with more cholesterol showed severer perturbations of fatty acid, carbohydrate and amino acid metabolism. In the HC group, the majority of significant elevations were identified for fatty acids, such as lauric acid, oleic acid, stearic acid, arachidonic acid, docosahexaenoic acid and cerotic acid. Reduced levels of glucose were also observed. Although there was a marked decrease in proline and tryptophan, as well as an elevation of glutamine, no statistical differences for the other amino acids were observed. It was interesting to find that increased dietary cholesterol in the EHC group not only intensified the fluctuation of metabolites observed in the HC group, but also led to greater variation of more metabolites, especially for amino acids. In detail, reduced levels of methionine, phenylalanine and tyrosine, and elevation of myo-inositol, γ-tocopherol, linoleic acid and α-linolenic acid were observed besides those mentioned above after high-cholesterol dietary treatment. Furthermore, the increase of relative amounts of linoleic acid, oleic acid, arachidonic acid and γ-tocopherol, and the decrease of phenylalanine and tyrosine in the EHC group contributed most to the differentiation between the EHC and HC groups.

Relationship between biochemical parameters and endogenous metabolites

It is of great interest to correlate biochemical parameters and levels of the potential markers. As shown in Table 2, the changes of foam cell areas were positively correlated with several metabolites including glucose, tyrosine, arachidonic acid, γ-tocopherol and cerotic acid (assessed by Pearson correlation coefficient).

Table 1. Fold change of serum metabolites characterizing hypercholesterolaemia–early atherosclerosis induced by a high-cholesterol diet[a].

		Fold change		
No.	Identified metabolites	HC/control	EHC/control	EHC/HC
1	2-hydroxy-butanoic acid	2.36[b]	3.23[d]	1.37
2	Methionine	–	0.84[b]	0.82
3	Proline	0.88	0.72[b]	–
4	Phenylalanine	–	0.83[b]	0.79[b]
5	Lauric acid	15.29[d]	20.78[c]	1.36
6	Glutamine	1.50[c]	1.75[d]	–
7	Glucose	0.52[c]	0.82[b]	1.58[b]
8	Tyrosine	–	0.72[b]	0.71[c]
9	Palmitic acid	–	1.31[b]	–
10	Myo-inositol	1.26	1.34[b]	–
11	α-Linolenic acid	–	1.31[b]	1.28
12	Linoleic acid	–	1.59[b]	1.40
13	Oleic acid	1.45[b]	1.79[b]	1.23
14	Tryptophan	0.45[c]	0.61[c]	1.32
15	Stearic acid	1.43[b]	1.67[c]	–
16	Arachidonic acid	2.19[c]	2.86[d]	1.30[d]
17	Myo-inositol-1-phosphate	1.95	1.83[b]	–
18	Docosahexaenoic acid	1.54	1.47[b]	–
19	γ-Tocopherol	2.36	6.87[b]	2.90[b]
20	Cerotic acid	3.15[b]	5.40[c]	1.71
21	Cholesterol	94.95[b]	94.03[c]	–

[a]Relative fold changes (high-cholesterol (HC) group to control group, extra-high cholesterol (EHC) group to control group, EHC group to HC group) at the 12-week time point. Control, $n=8$; HC, $n=7$; EHC, $n=6$.

[b]Correlation is significant at the 0.05 level; [c]correlation is significant at the 0.01 level; [d]correlation is significant at the 0.001 level (two-tailed Student's *t*-test); –, no significant change.

Table 2. Pearson correlation analysis between serum lipids levels, foam cell areas and some endogenous metabolites of hamsters fed a high-cholesterol diet.

	Foam cells area		TC		TG		HDL-C		LDL-C	
Metabolites	Pearson correlation coefficients	*p*-Value	Pearson correlation coefficients	*p*-Value	Pearson correlation coefficients	*p*-Value	Pearson correlation coefficients	*p*-Value	Pearson correlation coefficients	*p*-Value
Phenylalanine	−0.334	0.265	−0.507	0.092	−0.598[a]	0.040	−0.459	0.133	−0.522	0.082
Lauric acid	0.255	0.401	0.476	0.118	0.652[a]	0.022	0.500	0.098	0.603[a]	0.038
Glucose	0.623[a]	0.023	0.352	0.262	0.245	0.443	0.458	0.135	0.336	0.285
Tyrosine	−0.593[a]	0.033	−0.570	0.053	−0.437	0.156	−0.508	0.092	−0.508	0.092
Palmitic acid	0.357	0.231	0.447	0.145	0.385	0.216	0.404	0.193	0.694[a]	0.012
Linoleic acid	0.401	0.174	0.615[a]	0.033	0.600[a]	0.039	0.787[b]	0.002	0.589[a]	0.044
Olic acid	0.357	0.231	0.327	0.300	0.387	0.214	0.578[a]	0.049	0.327	0.299
Arachidonic acid	0.668[a]	0.013	0.168	0.601	0.122	0.706	0.293	0.355	0.136	0.672
γ-Tocopherol	−0.654[a]	0.029	−0.351	0.321	−0.145	0.690	−0.456	0.185	−0.308	0.387
Cerotic acid	0.722[b]	0.005	0.155	0.631	0.143	0.657	0.336	0.286	0.112	0.730

TC, total cholesterol; TG, triglyceride; HDL-C, high-density lipoprotein cholesterol; LDL-C, low-density lipoprotein cholesterol.

[a]Correlation is significant at the 0.05 level; [b]correlation is significant at the 0.01 level; [c]correlation is significant at the 0.001 level (two-tailed).

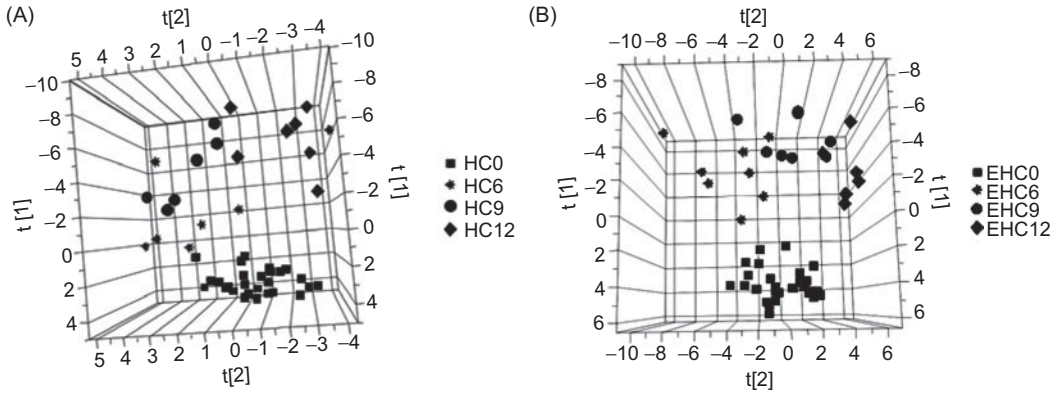

Figure 3. Partial least squares projection to latent structure and discriminant analysis (PLS-DA) score plots of the high-cholesterol (HC) group (A, three principal components (PCs), $R^2X=0.341$, $R^2Y=0.667$, $Q^2Y=0.433$) and the extra-high cholesterol (EHC) group (B, three PCs, $R^2X=0.355$, $R^2Y=0.654$, $Q^2Y=0.443$) over the whole experiment period. Both for the HC and EHC groups, clear movement of data points along with feeding a high-fat diet are shown, indicating that a high-fat diet has significant impact on metabonomics.

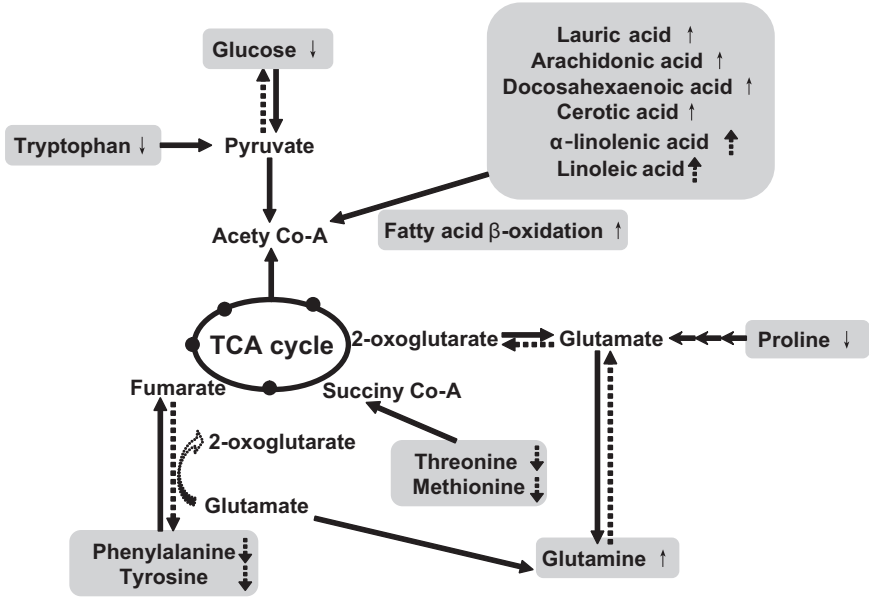

Figure 4. The metabolic pathways perturbed in the atherosclerosis model after induction with high-cholesterol food. The relative concentration of metabolites detected as increased or decreased during the whole experiments are indicated by adjoining arrows (↑/↓, increase/decrease in both the high-cholesterol (HC) and extra-high-cholesterol (EHC) groups; ↑/↓ increase/decrease only in the EHC group).

We also observed the correlation between linoleic acid and the four serum lipid parameters, although no significant correlation was observed between glucose, tyrosine, rachidonic acid, γ-tocopherol and cerotic acid and the four serum lipid parameters, respectively. The variation of phenylalanine was positively correlated with TG, and there was a positive correlation between lauric acid and TG, HDL-C, palmitic acid and LDL-C, olic acid and HDL-C, respectively.

Time-dependent metabolic effect in serum

Because the hamsters in the control groups were fed with a standard diet, and the serum metabolic profile of these control animals was stable and constant during the experiment, it in fact provided the baseline of the metabolite profile for the cholesterol-fed hamsters. On the other hand, the other two groups fed with a hypercholesterolaemic diet show a metabolic variation describing the process of hypercholesterolaemia to early atherosclerosis. In detail, by means of PCA and PLS-DA, GC/TOF-MS data of serum following two doses of cholesterol induction from 0 to 12 weeks was processed. The score plots showed time-dependent movement of the process (Figure 3A and B). The dots at different time points of the two groups were distinctly far away from the samples before cholesterol induction and in the Con group. It is shown in the score plots that the EHC samples at week 6 were obviously

distant from those at week 0 (Figure 3B), while in the HC group, samples at week 6 were not so far away from samples before cholesterol induction (Figure 3A). Statistical analysis of the data identified many metabolites (Figure 4). In particular, remarkable elevation of fatty acids, including lauric acid, arachidonic acid, docosahexaenoic acid, cerotic acid and glutamine were observed from 0 to 12 weeks in both the HC and EHC groups. Glucose, proline and tryptophan showed the opposite trend – decreased levels in both of the groups. Yet, the levels of phenylalanine, tyrosine, threonine, methionine, α-linolenic acid and linoleic acid increased in the EHC group while no statistical difference was observed between the HC group and the control group.

Discussion

Metabonomics may be a promising tool for identifying biomarkers that characterize the process from hypercholesterolaemia to atherosclerosis in order for a better understanding of the development of atherosclerosis resulting from food intake. In the current study, hamsters, instead of SD rats, were selected as the model animal as hamsters are not only more susceptible to diet-induced atherosclerosis than SD rats (data not shown), but also have similar plasma lipoprotein distributions to humans (Nistor et al. 1987). In general, humans take in an average of 3–5 mg cholesterol kg^{-1} body wt daily. This is an amount of sterol equal to about 50% of the cholesterol synthesized each day. A comparable dose of dietary cholesterol in hamsters would be about 20 mg cholesterol kg^{-1} body wt daily. A rigorous cholesterol challenge in either case would come from a diet formulated with a cholesterol intake of 5–10 times their daily synthesis rate. In hamsters, such a load is achieved with dietary cholesterol concentrations of about 0.1–0.3% (Kris-Etherton & Dietschy 1997). Therefore, our studies used 0.3% cholesterol for the HC diet and 0.8% cholesterol in the EHC diet.

Although the total serum cholesterol level did not change significantly from week 6 to week 12 following cholesterol induction, remarkable metabolic variations were observed during this process from hypercholesterolaemia to early atherosclerosis. Due to the formation of hypercholesterolaemia at week 6 and early atherosclerosis at week 9 in EHC group hamsters, the score plots showed and characterized metabolic variations from hypercholesterolaemia to early atherosclerosis, suggesting that development of the process was faster with a higher cholesterol diet. The elevation of free fatty acids strongly indicates perturbation of lipid metabolism, which can be explained as the response of hamsters to cholesterol-induced atherosclerosis (Nistor et al. 1987). The increase levels of lauric acid and palmitic acid may be indexes for the elevation of plasma LDL-C level. It has been shown that lauric acid and palmitic acid can accumulate in the liver and suppress hepatic LDL receptor activity through redistribution of intracellular cholesterol pools (Daumerie et al. 1992), and further enhance the formation of LDL-C (Woollett et al. 1992). In this study, the diet-dependent increase of LDL-C level was concurrent with those of lauric acid and palmitic acid levels.

Antoku et al. (2000) reported that elevation of cerotic acid was closely associated with atherosclerosis-related diseases. Cerotic acid is a saturated long-chain fatty acid (VLFA), and can therefore affect membrane receptor functions, which has been shown to be related to the atherogenic processes in vascular endothelial cells, endothelial cells and smooth muscle cells. To date, it is still not clear how cerotic acid in cell membranes participates in the atherosclerotic processes. In our model, cerotic acid levels were slightly higher in week 6 compared with baseline, and increased remarkably in the following 6 weeks for the EHC hamsters. This indicates that cholesterol feeding for the latter 6 weeks played a key role in the formation of atherosclerosis. In addition, elevated concentrations of linoleic acid and oleic acid were observed in hamster serum after feeding with a cholesterol diet. It has been shown that elevated concentrations of linoleic acid and oleic acid in serum may enhance the rate of synthesis of lipids in normal and atherosclerotic tissue, and thus exacerbate the accumulation of lipids, contributing to the development of atherosclerosis (Sato et al. 1985).

Interestingly, loading of an extra-high diet of cholesterol (EHC group) strongly affected a number of amino acids, resulting in perturbation of amino acid metabolism, in addition to that of fatty acid and glucose metabolism. In this study, we observed a remission of the metabolic perturbation once the amount of cholesterol in the diet was reduced. The result was consistent with a previous report showing a dose-dependent effect of dietary cholesterol (Kleemann et al. 2007). Levels of many amino acids, such as threonine, methionine, phenylalanine and tyrosine decreased after cholesterol induction. Yet glutamine was the only amino acid that increased, which may be attributed to the inhibition of glutamine metabolism by cholesterol (Lescano-De-Souza and Curi 1999). Because of the complexity of amino acid metabolism pathways, the pathophysiological mechanism induced by dietary cholesterol needs further clarification.

In conclusion, GC/MS- and MVSA-based metabonomics has been successfully applied to investigate molecular responses to cholesterol in hamsters. Dose- and time-dependent metabolic variation was well differentiated to characterize the process from hypercholesterolaemia to early atherosclerosis. The identified

biomarkers suggested that the perturbation of lipid and amino acid metabolism is involved in this process. The present study provided evidence that GC/MS-based metabonomics can be used to identify the metabolic variation associated with early atherosclerosis, and further suggests it is a promising tool to approach the pathophysiological processes of diseases by providing novel information on endogenous compounds.

Acknowledgements

The authors thank Professor Lin Xie and graduate students, Shihai Yan, Nanqi Shao and Enze Guan, for their technical assistance. We also thank Beth Shoshana Pecora, Virginia Commonwealth University, for the revision of the paper. This study was financially supported by the National Nature Science Fund (30572228 and 30630076), the Jiangsu Nature Science Fund (BK2005098), and the Jiangsu International Cooperation Fund (BZ2006049).

***Declaration of interest*:** The authors report no conflicts of interest. The authors alone are responsible for the content and writing of the paper.

References

A JY, Trygg J, Gullberg J, Johansson A, Jonsson P, Antti H, Marklund S, Moritz T. (2005). Extraction and GC/MS analysis of the human blood plasma metabolome. Anal Chem 77:8086–94.

Allain CC, Poon LS, Chen CS, Richmond W, Fu PC. (1974). Enzymatic determination of total serum cholesterol. Clin Chem 20:470–5.

Antoku Y, Tsukamoto K, Miyoshi Y, Nagino H, Anezaki M, Suwa K, Narabe Y. (2000). Correlations of elevated levels of hexacosanoate in erythrocyte membranes with risk factors for atherosclerosis. Atherosclerosis 153:169–73.

Bijnens AP, Lutgens E, Ayoubi T, Kuiper J, Horrevoets AJ, Daemen MJAP. (2006). Genome-wide expression studies of atherosclerosis: critical issues in methodology, analysis, interpretation of transcriptomics data. Arterioscler Thromb Vasc Biol 26:1226–35.

Brindle JT, Antti H, Holmes E, Tranter G, Nicholson JK, Bethell HWL, Clarke S, Schofield, PM, Mckilligin E, Mosedale DE, Grainger DJ. (2002). Rapid and noninvasive diagnosis of the presence and severity of coronary heart disease using 1H-NMR-based metabonomics. Nat Med 8:1439–44.

Bucolo G, David H. (1973). Quantitative determination of serum triglycerides by the use of enzymes. Clin Chem 36:476–82.

Daumerie CE, Woollett LA, Dietschy JM. (1992). Fatty acids regulate hepatic low density lipoprotein receptor activity through redistribution of intracellular cholesterol pools. Proc Natl Acad Sci USA 89:10797–801.

Dumas ME, Barton RH, Toye A, Cloarec O, Blancher C, Rothwell A, Fearnside J, Tatoud R, Blanc V, Lindon J, Mitchell SC, Holmes E, McCarthy MI, Scott J, Gauguier D, Nicholson JK. (2006). Metabolic profiling reveals a contribution of gut microbiota to fatty liver phenotype in insulin-resistant mice. Proc Natl Acad Sci USA 103:1511–16.

Eriksson L, Johansson E, Kettaneh-Wold N, Wold S. (2001). Multi- and megavariate data analysis principles and applications. Umea, Sweden: Umetrics Academy, Umetrics AB.

Hui DY. (2003). HIV protease inhibitors and atherosclerosis. J Clin Invest 111:317–18.

Jonsson P, Johansson AI, Gullberg J, Trygg J, A JY, Grung B, Marklund S, Sjöström M, Antti H, Moritz T. (2005). High-throughput data analysis for detecting and identifying differences between samples in GC/MS-Based metabolomic analyses. Anal Chem 77:5635–42.

Kenny LC, Dunn WB, Ellis DI, Myers J, Baker PN, Kell DB. (2005). Novel biomarkers for pre-eclampsia detected using metabolomics and machine learning. Metabolomics 1:227–34.

Kleemann R, Verschuren L, Erk MJ, Nikolsky Y, Cnubben NHP, Verheij ER, Smilde AK, Hendriks HFJ, Zadelaar S, Smith GJ, Kaznacheev V, Nikolskaya T, Melnikov A, Hurt-Camejo E, Greef J, Ommen B, Kooistra T. (2007). Atherosclerosis and liver inflammation induced by increased dietary cholesterol intake: a combined transcriptomics and metabolomics analysis. Genome Biol 8:R200.

Kris-Etherton PM, Dietschy J. (1997). Design criteria for studies examining individual fatty acid effects on cardiovascular disease risk factors: human and animal studies. Am J Clin Nutr 65 (Suppl.):1590S–6S.

Lahoz C, Mostaza, JM. (2007). Atherosclerosis as a systemic disease. Rev Esp Cardiol 60:184–95.

Lescano-De-Souza AJ, Curi R. (1999). Cholesterol inhibits glutamine metabolism in LLC WRC256 tumour cells but does not affect it in lymphocytes: possible implications for tumour cell proliferation. Cell Biochem Funct 17:223–38.

Lusis AJ. (2000). Atherosclerosis. Nature 407:233–41.

Mayr M, Chung Y, Mayr U, Yin X, Ly L, Troy H, Fredericks S, Hu Y, Griffiths JR, Xu Q. (2005). Proteomic and metabolomic analyses of atherosclerotic vessels from apolipoprotein E-deficient mice reveal alterations in inflammation, oxidative stress, and energy metabolism. Arterioscler Thromb Vasc Biol 25:2135–42.

Nicholson J, Lindon, J, Holmes E. (1999). 'Metabonomics': understanding the metabolic responses of living systems to pathophysiological stimuli via multivariate statistical analysis for biological NMR spectroscopic data. Xenobiotica 29:1181–9.

Nistor A, Bulla A, Filip DA, Radu A. (1987). The hyperlipidemic hamster as a model of experimental atherosclerosis. Atherosclerosis 68:159–73.

Sabatine MS, Liu E, Morrow DA, Heller E, McCarroll R, Wiegand R, Berriz GF, Roth FP, Gerszten RE. (2005). Metabolomic identification of novel biomarkers of myocardial ischemia. Circulation 112:3868–75.

Sato T, Saito T, Yoshinaga K. (1985). The chemical composition of the thoracic aorta in diabetic and non-diabetic rats. Tohoku J Exp Med 147:357–64.

Steinberg D. (2002). Atherogenesis in perspective: hypercholesterolemia and inflammation as partners in crime. Nat Med 8:1211–17.

Sung HJ, Ryang YS, Jang SW, Lee CW, Han KH, Ko J. (2006). Proteomic analysis of differential protein expression in atherosclerosis. Biomarkers 11:279–90.

Trygg J, Lundstedt T. (2007). Chemometrics techniques for metabonomics. J Proteome Res 6:469–79.

Tuomisto TT, Binder BR, Ylä-Herttuala S. (2005). Genetics, genomics and proteomics in atherosclerosis research. Ann Med 37:323–32.

Weingand KW, Daggy BP. (1990). Quantitation of high-density lipoprotein cholesterol in plasma from hamsters by differential precipitation. Clin Chem 36:575.

Wold S. (1978). Cross-validatory estimation of the number of components in factor and principal components models. Technometrics 20:397–405.

Woollett LA, Spady DK, Dietschy JM. (1992). Regulatory effects of the saturated fatty acids 6:0 through 18:0 on hepatic low density lipoprotein receptor activity in the hamster. J Clin Invest 89:1133–41.

Yi LZ, Yuan DL, Che ZH, Liang YZ, Zhou ZG, Gao HY, Wang YM. (2008). Plasma fatty acid metabolic profile coupled with uncorrelated linear discriminant analysis to diagnose and biomarker screening of type 2 diabetes and type 2 diabetic coronary heart diseases. Metabolomics 4:30–8.